ISSN 1674-1056
http://cpb.iphy.ac.cn
http://iopscience.iop.org/cpb
中国物理 B
Chinese Physics
中国物理 Chinese Physics B

## Highly-sensitive NO, $NO_2$, and $NH_3$ measurements with an open-multipass cell based on mid-infrared wavelength modulation pectroscopy

Xiang Chen(陈祥), Chen-Guang Yang(杨晨光), Mai Hu(胡迈), Jian-Kang Shen(沈建康), Er-Chao Niu(牛二超), Zhen-Yu Xu(许振宇), Xue-Li Fan(范雪丽), Min Wei(魏敏), Lu Yao(姚路), Ya-Bai He(何亚柏), Jian-Guo Liu(刘建国), Rui-Feng Kan(阚瑞峰)
**Citation:**Chin. Phys. B . 2018, 27(4): 040701. **doi:** 10.1088/1674-1056/27/4/040701

Journal homepage: http://cpb.iphy.ac.cn; http://iopscience.iop.org/cpb

**What follows is a list of articles you may be interested in**

---

## Optical sensors based on the NiPc–CoPc composite films deposited by drop casting and under the action of centrifugal force

Noshin Fatima, Muhammad M Ahmed, Khasan S Karimov, Zubair Ahmad, Fahmi Fariq Muhammad
Chin. Phys. B . 2017, 26(6): 060704. **doi:** 10.1088/1674-1056/26/6/060704

## Room temperature $NO_2$-sensing properties of hexagonal tungsten oxide nanorods

Yaqiao Wu(武雅乔), Ming Hu(胡明), Yuming Tian(田玉明)
Chin. Phys. B . 2017, 26(2): 020701. **doi:** 10.1088/1674-1056/26/2/020701

## Ultralow detection limit of giant magnetoresistance biosensor using $Fe_3O_4$-graphene composite nanoparticle label

Jie Xu(徐洁), Ji-qing Jiao(焦吉庆), Qiang Li(李强), Shan-dong Li(李山东)
Chin. Phys. B . 2017, 26(1): 010701. **doi:** 10.1088/1674-1056/26/1/010701

## High signal-to-noise ratio sensing with Shack-Hartmann wavefront sensor based on auto gain control of electron multiplying CCD

Zhao-Yi Zhu(朱召义), Da-Yu Li(李大禹), Li-Fa Hu(胡立发), Quan-Quan Mu(穆全全), Cheng-Liang Yang(杨程亮), Zhao-Liang Cao(曹召良), Li Xuan(宣丽)
Chin. Phys. B . 2016, 25(9): 090702. **doi:** 10.1088/1674-1056/25/9/090702

## Calibration chain design based on integrating sphere transfer radiometer for SI-traceable on-orbit spectral radiometric calibration and its uncertainty analysis

Wei-Ning Zhao(赵维宁), Wei Fang(方伟), Li-Wei Sun(孙立微), Li-Hong Cui(崔立红), Yu-Peng Wang(王玉鹏)
Chin. Phys. B . 2016, 25(9): 090701. **doi:** 10.1088/1674-1056/25/9/090701

---

# Highly-sensitive NO, $NO_2$, and $NH_3$ measurements with an open-multipass cell based on mid-infrared wavelength modulation spectroscopy*

Xiang Chen(陈祥)[1,2], Chen-Guang Yang(杨晨光)[1], Mai Hu(胡迈)[1], Jian-Kang Shen(沈建康)[3], Er-Chao Niu(牛二超)[3], Zhen-Yu Xu(许振宇)[1], Xue-Li Fan(范雪丽)[1], Min Wei(魏敏)[1,2], Lu Yao(姚路)[1], Ya-Bai He(何亚柏)[1], Jian-Guo Liu(刘建国)[1], and Rui-Feng Kan(阚瑞峰)[1,†]

[1] *Key Laboratory of Environmental Optics and Technology, Anhui Institute of Optics and Fine Mechanics, Chinese Academy of Sciences, Hefei* 2300314, *China*

[2] *University of Science and Technology of China, Hefei* 230022, *China*

[3] *Jiangsu Environmental Monitoring Center, Nanjing* 210036, *China*

(Received 24 October 2017; revised manuscript received 3 January 2018; published online 10 March 2018)

A compact prototype based on mid-infrared wavelength modulation spectroscopy (WMS) is developed for the simultaneous monitoring of NO, $NO_2$, and $NH_3$ in the urban area. Three quantum cascade lasers (QCLs) with central frequencies around 1900.0 $cm^{-1}$, 1600.0 $cm^{-1}$, and 1103.4 $cm^{-1}$ are used for NO, $NO_2$, and $NH_3$ detections, respectively, by time-division multiplex. An open-path multi-pass cell of 60-m optical path length is applied to the instrument for high sensitivity and reducing the response time to less than 1 s. The prototype achieves a sub-ppb detection limit for all the three target gases with an average time of about 100 s. The instrument is installed in the Jiangsu environmental monitoring center to conduct performance tests on ambient air. Continuous 24-hour measurements show good agreement with the results of a reference instrument based on the chemiluminescence technique.

**Keywords:** wavelength modulation spectroscopy, optical sensing, atmospheric monitoring, time division multiplexing, quantum cascade laser, mid-infrared laser spectroscopy

**PACS:** 07.07.Df, 33.20.–t, 42.55.Px, 42.62.–b **DOI:** 10.1088/1674-1056/27/4/040701

## 1. Introduction

As the precursors of secondary fine particulate matters, NO, $NO_2$, and $NH_3$ in the air have been causing global environmental issues. $NO_x$ participates in a chain reaction that destroys the protective stratospheric ozone layer, resulting in an increase of ultraviolet radiation reaching the surface of the Earth.[1] Also, $NO_x$ promotes acid rain that causes soil acidification and affects the growth of plants.[2] Moreover, $NO_x$ plays an important role in forming photochemical smog.[3] Therefore, it is essential to reliably measure the $NO_x$ concentration in ambient air, as one of the most abundant nitrogen-containing molecules, ammonia, has important effects on atmospheric chemistry and the environment. The major ingredient is alkaline gas, and therefore it plays an important role in neutralizing the acidic gases and forming the particulate matters. However, $NH_3$ adsorption onto the sampling manifolds can result in significant discrepancies between the measured and actual concentrations.[4] Open-path arrangements can help to make accurate measurements without being affected by adsorption.[5,6]

In recent years, the detecting of NO, $NO_2$, and $NH_3$ based on infrared WMS[7–10] has been widely studied for industrial processes, environmental monitoring and medical diagnoses. For example, a quantum cascade laser (QCL)[11,12] with a center wavelength $\sim$ 5263 nm was used to detect NO emission.[2] With a resolution of line strength, a resolution about 2 ppm was realized and the relative error was less than 3%. In order to estimate the NO and $NO_2$ background level in the free troposphere, a QCL-based absorption spectrometer was employed at the high-altitude site Jungfraujoch (3850 m a.s.l) in Switzerland.[13] The precisions of 10 ppt and 3 ppt for NO and $NO_2$ were achieved under field conditions with 180-s averaging time, resepectively. The linear dynamic range of the instrument for both species increased up to 45 ppb. Also, it is essential to measure NO and its metabolites in various body compartments to enhance our understanding of biology. Wang *et al.* presented a mid-IR Faraday rotation spectrometer for detecting the NO isotopes with detection limits of 3.72 ppbv/$Hz^{1/2}$ for $^{14}NO$ and 0.53 ppbv/$Hz^{1/2}$ for $^{15}NO$, respectively.[14] Generally, a single-laser system is less complex and consumes less power than systems using multiple laser modules. Jagersk *et al.* presented the practical real-

*Project supported by the National Key Scientific Instrument and Equipment Development, China (Grant No. 2014YQ060537) and the National Key Research and Development Program, China (Grant No. 2016YFC0201103).

†Corresponding author. E-mail: kanruifeng@aiofm.ac.cn

© 2018 Chinese Physical Society and IOP Publishing Ltd 

ization of such a pulsed QCL dual-wavelength setup, which emitted single-mode radiation at 1600 $cm^{-1}$ and 1900 $cm^{-1}$ and was suited for simultaneously detecting NO and $NO_2$.[15] In industrial processes, the $NO_x$ emission in exhaust gasses was strictly restricted, whereas ammonia was widely used in flue gas treatment for de$NO_x$ applications. Therefore, a highly sensitive setup based on near-infrared lasers for the detection of excess $NH_3$ has been investigated.[16] The extractive gas cell was heated to a temperature of 180 °C to avoid condensing the moisture and sticking the ammonia molecules. For an ammonia breath sensor, using absorption lines located at the near-infrared absorption band may not satisfy the demand for detection limit. A calibration-free ammonia sensor using a QCL with the WMS technique was demonstrated for monitoring the ammonia in exhaled breath.[17] The minimum detectable ammonia mole fraction was found to be 7 ppb with a 76.45-m long extractive multi-pass gas cell. Compared with the extractive type, the open-path sensor configuration minimized sampling artifacts associated with $NH_3$ surface adsorption onto the inlet tubing.[18] This open-path sensor has a sensitivity and noise-equivalent limit of 0.15-ppbv $NH_3$ at 10 Hz.

To be able to do further research on the formation of secondary fine particulate matters, we report the development of a QCL-based instrument for monitoring NO, $NO_2$, and $NH_3$ in the open air. Three absorption lines located at 1900.0 $cm^{-1}$, 1600.0 $cm^{-1}$, and 1103.4 $cm^{-1}$ were selected for detecting NO, $NO_2$, and $NH_3$ respectively, where the line strengths were two orders stronger than those in the near-infrared absorption region. In contrast to closed-path systems, our non-destructive open-path design minimized the challenges of sampling artifacts and provided a fast time response. The time division multiplexing technology and second harmonic analysis with WMS can be used to simultaneously detect NO, $NO_2$, and $NH_3$ at a sub-ppb level. To test its reliability and long-term operation, the prototype was installed in the Jiangsu environmental monitoring center and compared with the measuring instrument based on chemiluminescence in the center.

## 2. Theory and absorption line selection

### 2.1. WMS principles

When a QCL injection current is modulated by a sinusoidal modulation signal, the laser frequency $\nu(t)$ and output intensity $I(t)$ can be expressed as

$$\nu(t) = \bar{\nu} + a\cos(\omega t), \tag{1}$$

$$I(t) = \overline{I_0} + i_1\cos(\omega t + \psi_1) + i_2\cos(2\omega t + \psi_2), \tag{2}$$

where $\bar{\nu}$ is the center laser frequency, $\overline{I_0}$ is the average laser intensity, $a$ is the amplitude of frequency modulation, $i_1$ and $i_2$ are the linear amplitude and the nonlinear amplitude of the intensity modulation, respectively, $\omega$ is the angular modulation frequency, while $\psi_1$ and $\psi_2$ are the phase shifts of the linear term and the nonlinear term, respectively. In most of the situations, $i_2$ is much smaller than $i_1$ and their effects of nonlinearities can be ignored.[19] When the modulated laser radiation passed through the gas sample, the transmittance was given by the Beer–Lambert relation

$$\tau(\nu,\nu 0) = \exp\left(-S(T)PXL\varphi(\nu,\nu 0)\right), \tag{3}$$

where $S(T)$ is the absorption line strength at temperature $T$, $P$ is the pressure, $X$ is the mole fraction of absorbing species, $L$ is the optical path length, and $\varphi(\nu,\nu_0)$ is the lineshape function. For an optically thin sample, the transmittance can be described approximately as

$$\tau(\nu,\nu 0) \approx 1 - S(T)PXL\varphi(\nu,\nu 0). \tag{4}$$

Expand the transmittance in Fourier series of laser angular modulation frequency and its harmonics $k\omega$

$$\tau(\nu(t),\nu 0) = \sum_{k=0}^{\infty} H_k(\bar{\nu},\nu_0,a)\cos(k\omega t), \tag{5}$$

and combine with simplified Beer–Lambert relation for weak absorption, then $H$ terms will be written as

$$H_0(\bar{\nu},\nu_0,a) = \frac{S(T)PXL}{2\pi}\int_{-\pi}^{\pi}\varphi(\bar{\nu},\nu_0)\,\mathrm{d}\theta, \tag{6}$$

$$H_k(\bar{\nu},\nu_0,a) = \frac{S(T)PXL}{\pi}\int_{-\pi}^{\pi}\varphi(\bar{\nu},\nu_0)\cos k\theta\,\mathrm{d}\theta. \tag{7}$$

In the experiment, a digital lock-in amplifier with appropriate parameters was used to attain the first and second (i.e., $1f$ and $2f$) harmonic signal of the transmitted light intensity through the gas sample. By normalizing the $2f$ signal against the magnitude of the $1f$ signal, the dependence on laser intensity was eliminated. To a good approximation, the amplitude of the normalized $2f$ signal was found to be

$$I_{2f/1f} \propto S(T)PXL. \tag{8}$$

After the line strength, the air pressure and optical path length have been predetermined, and the gas concentration can be acquired based on Eq. (8). For long-term monitoring measurements, the ambient temperature $T$ and pressure $P$ are recorded for calculating the line strength and the mole fraction $X$ value.

### 2.2. Absorption line selection

Since the detection was performed on ambient air with an open-path setup, water vapor, carbon dioxide and other species in the air may cause interferences due to their overlapping absorption features or pressure broadening effects. Therefore, spectral features in the ranges of 1900.0 $cm^{-1}$, 1600.0 $cm^{-1}$, and 1103.4 $cm^{-1}$ were selected for NO, $NO_2$, and $NH_3$, where their absorption features overlap with the minimum of the adjacent interfering gas absorption feature, and the line strength

was relatively strong. To demonstrate the feasibility further, the detailed simulations of absorption spectra of NO, $NO_2$, and $NH_3$, together with typical ambient mixing ratios of atmospheric absorbers were performed. Figure 1 shows the spectra simulated based on HITRAN databases for 10-ppb NO, 40-ppb $NO_2$, 15-ppb $NH_3$, 80-ppb $O_3$, 400-ppm $CO_2$, 1800-ppb $CH_4$, 5-ppb $SO_2$, and 2.0% $H_2O$ at 296 K and 1 atm (1 atm = $1.01325\times10^5$ Pa) for a 60-m optical path length. In the region of 1900 $cm^{-1}$, the NO absorption feature is a superposition of five absorption transitions, and the major influence comes from $CO_2$ and $H_2O$. For $NO_2$ and $NH_3$ absorption lines near 1600.0 $cm^{-1}$ and 1103.4 $cm^{-1}$, respectively, the $H_2O$ lines still have a remarkable influence. To analyze the influences of $H_2O$, $CO_2$ and other atmospheric gases quantitatively, the second harmonic signals were simulated with the same conditions and are presented in Fig. 2. From the results, 2.0% $H_2O$ along with 400 ppm $CO_2$ will result in 1.5% deviation of the amplitude of NO (0.15 ppb). The amplitudes of $NO_2$ and $NH_3$ would vary about 0.7% (0.28 ppb) and 0.18% (0.03 ppb), respectively, while $H_2O$ changes from 0.0% to 2.0%. Other atmospheric species such as $O_3$, $CH_4$, and $SO_2$ can be neglected for the retrieval of second harmonic signals. In the ambient monitoring experiment, the average ambient concentrations of $H_2O$ and $CO_2$ for a given time period were used to calculate the background $1f$-normalized $2f$ signals based on the QCLs output. These $H_2O$ and $CO_2$ background $1f$-normalized $2f$ signals were then subtracted from the demodulated measurement signals to remove their contribution. A typical daily concentration fluctuation of $CO_2$ in the air is about 50 ppm. The concentration of $H_2O$ can be detected by a hygrometer and the short-term fluctuation was typically a few hundred ppm. Based on the simulation, the concentration fluctuations of $CO_2$ and $H_2O$ in air have much smaller influences on measurements of NO, $NO_2$, and $NH_3$ than their system detection limits ($< 0.1$ ppb). The detailed simulation analysis confirms that absorption lines located at 1900.0 $cm^{-1}$, 1600.0 $cm^{-1}$ and 1103.4 $cm^{-1}$ are appropriate for detecting the NO, $NO_2$, and $NH_3$ with open-path cells.

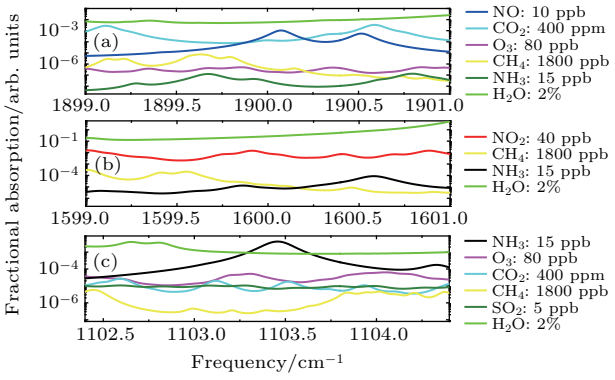



**Fig. 1.** (color online) Direct absorption HITRAN simulations of (a) NO, (b) $NO_2$, and (c) $NH_3$, with typical ambient mixing ratios of atmospheric absorbers, based on 60-m path length, 296 K, 1 atm.

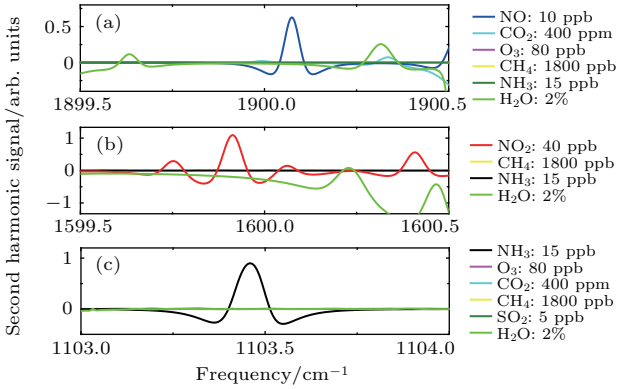



**Fig. 2.** (color online) Second harmonic spectra of (a) NO, (b) $NO_2$, and (c) $NH_3$, with typical ambient mixing ratios of atmospheric absorbers calculated based on 60-m path length, 296 K, 1 atm.

## 3. Instrument setup

The schematic diagram of the open-path sensor is shown in Fig. 3. The open-path design was optimized for field portability with a 131 cm×41 cm×35 cm sensor head and a 49 cm×50 cm×62 cm control unit. The total weight of the sensor is 68 kg. The quantum cascade lasers (Hamamatsu Lasers), were installed on the surface of Peltier devices with excellent heat dissipation controlled by low-noise current drivers (Wavelength electronics, PLD1250) and precision temperature controllers (Wavelength electronics, PTC10K-CH), respectively. Furthermore, the temperature of the enclosure of QCLs and drivers were controlled by fans, along with Peltier devices with high-efficiency temperature controllers (Analog Technologies, TECA1-XV) to achieve high stability in field conditions.

In the experiment three 50-Hz-frequency time division multiplexing sawtooth ramp signals superimposed with a 30-kHz-frequency sinusoidal signal were used to modulate laser injection currents. The ramp and modulation signals were generated by a data acquisition device (DAQ, NI-USB 6363, 16-bit resolution). Three QCLs output beams were combined by wedged dielectric beam splitters ($R > 93\%$ and $T > 90\%$ on both sides), and passed through a 25-cm-long reference gas cell equipped with wedged $CaF_2$ windows before being injected into an open-air multi-pass cell. By using wedged beam splitters, no optical interferences would be formed. The reflectors were coated with gold film ($R > 99\%$). The multi-pass cell consisted of two 10.2-cm-diameter gold-coated spherical mirrors ($R > 99\%$), with a base length of 0.87 m, which could provide an optical path length of 60 m. A green indication light beam was used to guide optical beam path adjustments.

The output beams from the multi-pass cell were focused onto a room-temperature MCT photodiode (Vigo, PC-2TE) by an off-axis parabolic mirror ($f = 50.4$ mm) and fine adjustment was made to optimize the detector signal. Data acquisition of the detector output signal was performed by the same DAQ card with a sampling rate of 2 MHz and a resolution of

16 bits. The raw spectral signal was averaged over 50 scans to enhance the signal-to-noise ratio. In operation, digital lock-in processing of the acquired data can be performed in real time, which led to a response time of 1 s. Meanwhile, ambient temperature ($T$) and pressure ($P$) were recorded with measuring equipment (OMEGA, iBTHX). The measuring accuracies of temperature and pressure were 0.5 °C and 2 mbar (1 bar = $10^5$ Pa), respectively. The concentration detection responsivities of the instrument at $T$ and $P$ (see Eq. (8)) were obtained by multiplying its calibration values, which were measured at $T_0$ and $P_0$ (see Fig. 5), with the ratios of $S(T)/S(T_0)$ and $P/P_0$.

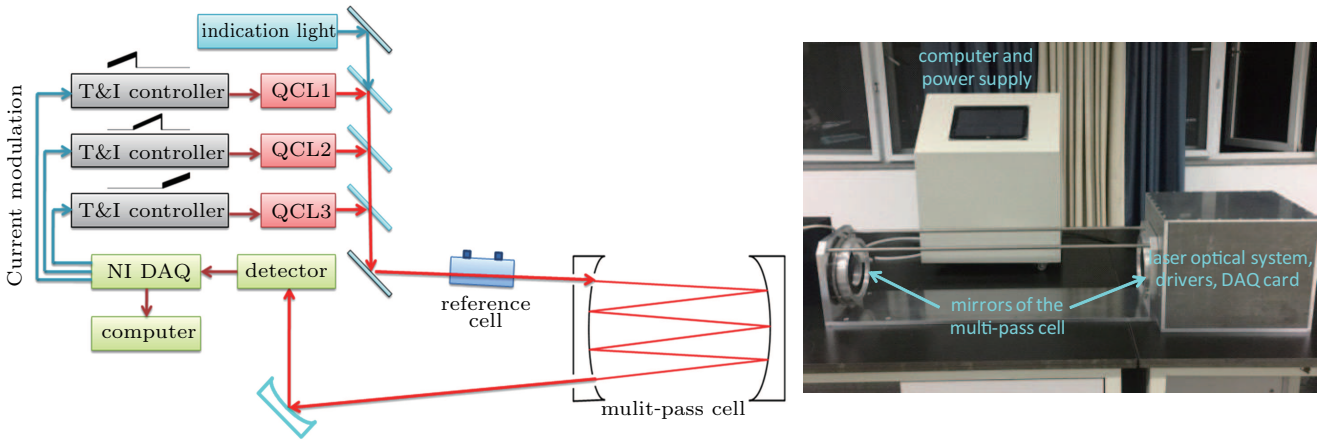



**Fig. 3.** (color online) Schematic diagram of an open-path instrument for atmospheric gas sensing, based on the wavelength modulation spectroscopy technique and mid-infrared quantum cascade lasers.

## 4. Experimental results and discussion

### 4.1. Modulation signal optimization and sensitivity calibration

The sweep cycle rate of time division multiplexing signals is interleaved at 50 Hz and the fast modulation frequency is at 30 kHz. When QCLs are not in the emitting state, their bias currents are set slightly below their thresholds without emitting any light or causing interference. This method of operating the laser current just below its threshold rather than turning off the current completely avoids rapidly declining the injection current and helps to achieve a longer operational lifespan for the lasers. In addition, the time division multiplexing technique reduces the average light-emitting time of QCLs as well as the produced heat, and improved the thermal stability of the system. Another reported approach is to modulate each of the lasers at different frequencies. This required complex signal demodulation also increases the photodetector's total amount of received light emitted by multiple lasers, which will contribute to higher noise.

Since the modulation depth varies with modulation voltage directly, an appropriate modulation voltage is required to maximize the $1f$-normalized $2f$ amplitudes of NO, $NO_2$, and $NH_3$. We investigate the modulation characteristics by using the fixed concentrations of NO, $NO_2$, and $NH_3$ in the 25-cm reference cell alternatively and by filling the enclosed open-path cell with pure $N_2$. The amplitudes of NO, $NO_2$, and $NH_3$ $1f$-normalized $2f$ signals at different modulation voltages are recorded in Fig. 4. Based on these results, the modulation amplitudes of 140 mV for NO, 120 mV for $NO_2$, and 240 mV for $NH_3$ are selected and used in the subsequent experiments. These correspond to modulation depths of 0.048 $cm^{-1}$, 0.062 $cm^{-1}$, and 0.10 $cm^{-1}$ for NO, $NO_2$, and $NH_3$, respectively.

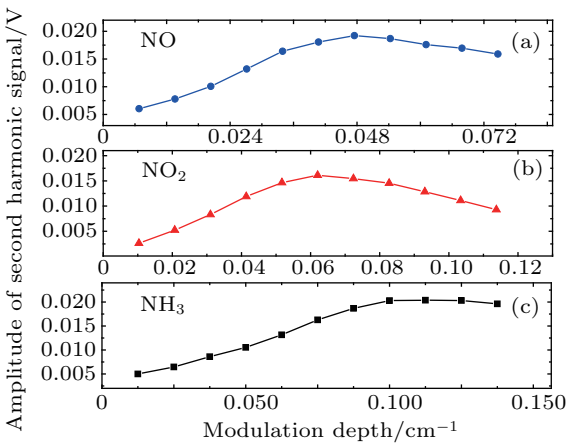



**Fig. 4.** (color online) $1f$-normalized $2f$ signal amplitudes of (a) NO, (b) $NO_2$, and (c) $NH_3$ at different modulation depths.

Due to the large volume of the 60-m-long multi-pass cell and the sticky characteristics of $NO_x$ and $NH_3$, serious deviations may be introduced when we calibrate this system directly with gas samples at a ppb level. According to the Specifications and Test Procedures for the Ambient Air Quality Continuous Automated Monitoring System promulgated by the Chinese Ministry of Environmental Protection,[20] the 2.5-cm-diameter short reference-gas cell can be used for accurate in-line calibration. While examining the responses of the system

at different concentrations of gas samples, the multi-pass cell is enclosed and purged with pure $N_2$ gas. After calibration is finished, the enclosure is removed and the reference cell is filled with pure $N_2$. For an open-path setup, this approach minimizes the calibration deviations and prevents the open-path cell from being contaminated.

The responses of the sensor system at different concentrations of gas samples are studied by using reference gas mixtures (Guangming Research & Design Institute of Chemical Industry, with 2% relative uncertainty). Pure $N_2$ and reference gas samples of NO (10 ppm, 20 ppm, 30 ppm, 40 ppm, 50 ppm), $NO_2$ (5 ppm, 15 ppm, 25 ppm, 35 ppm, 45 ppm), and $NH_3$ (10 ppm, 20 ppm, 30 ppm, 40 ppm, 50 ppm) are injected into the reference cell successively. Due to the characteristics of $NO_x$ and $NH_3$ strongly adsorbing the cell surface, an empirical relatively fast gas flow rate of 5 L/min is used to stabilize the cell surface in a short time of $\sim$5 min. The gas flow of each concentration is maintained for fifteen mins before acquiring stable $1f$-normalized $2f$ signals. The experimental data are recorded for five mins in order to obtain an accurate instrumental response. The peak values of $1f$-normalized $2f$ signals are calculated and the good linear relationships between gas concentration and peak value for different gases are observed as shown in Fig. 5.

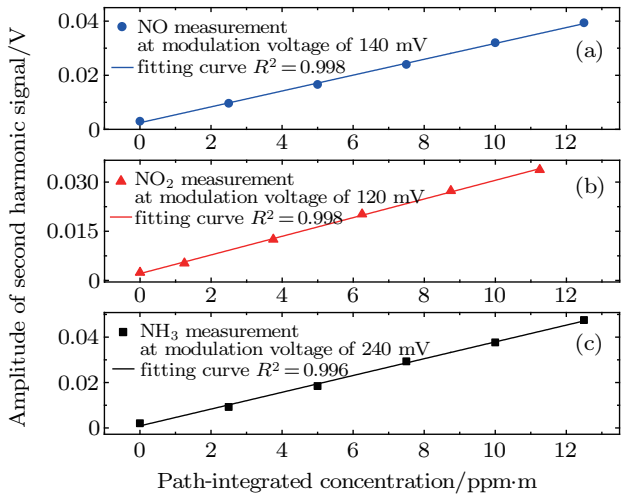



**Fig. 5.** (color online) Calibrations of the detection responsivity of the instrument for (a) NO, (b) $NO_2$, and (c) $NH_3$.

### 4.2. Allan deviation

The minimum detection limits (MDL) of the system for the three gases are investigated as a function of averaging measurement time. To remove the fluctuation influence derived from concentration fluctuations in the ambient air, a pure $N_2$ purge gas flow is used to fill the laser beam path including the reference cell and the enclosed open-path cell. Continuous measurement results with the three QCLs (for NO, $NO_2$, and $NH_3$, respectively) are recorded for 25 min with time-division multiplex at the 1-Hz cycle rate. Allan variance analysis[21–23] is performed and the results are plotted in Fig. 6, showing the precision of gas measurements as a function of the averaging time. As indicated in the figure, MDLs of 0.12 ppb for NO, 0.11 ppb for $NO_2$, and 0.11 ppb for $NH_3$ with optimum averaging times of 80 s, 150 s, and 100 s can be achieved with this setup. As the averaging time increases further, the detection limits start to degrade as shown in Fig. 6. The plots demonstrate 1-s detection limits of 0.96 ppb, 0.94 ppb, and 0.86 ppb for NO, $NO_2$, and $NH_3$ respectively. These similar detection limits for all three gases are just a coincidence despite differences in absorption line strength among the three gases and in operation characteristic among three corresponding QCLs. While the concentrations of NO, $NO_2$, and $NH_3$ molecules in the air fluctuate at a ppb level, this instrument is suitable for their environmental monitoring with a response time of 1 s.

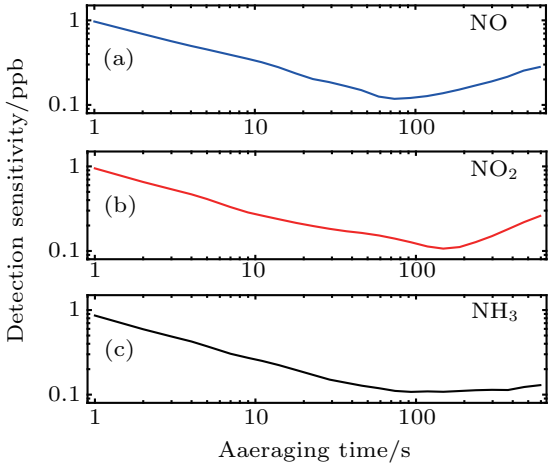



**Fig. 6.** (color online) Allan deviation plots of (a) NO, (b) $NO_2$, and (c) $NH_3$ detection sensitivity as a function of averaging time.

### 4.3. Wavelength stability

The wavelength stability of QCL is essential as severe wavelength drift may tune the target absorption lines outside of the scanning range. An active wavelength stabilization is an option, but would increase the system complexity and cost. We find that maintaining a high temperature stability is sufficient to minimize the wavelength drift. Since the wavelength drift correlates well with the temperature of the laser case and drivers, the precise temperature control is performed to suppress the drift. An example of $1f$-normalized $2f$ signals of ambient air recorded at 1 Hz is depicted in Fig. 7. The temperatures of laser shells and drivers are stabilized at $20 \pm 0.15$ °C and $25 \pm 1$ °C respectively with Peltier devices. The laser wavelength drifts as determined by the peak position of wavelength scan signals, which are recorded in Fig. 8, for 24 hours in the steps of 1 min. Based on the result, daily wavelength drift is minimized to less than 0.01 $cm^{-1}$. Therefore, the prototype is able to make measurements continuously without

any adjustment, as the laser wavelength drift changes within a small range of the absorption spectra profile.

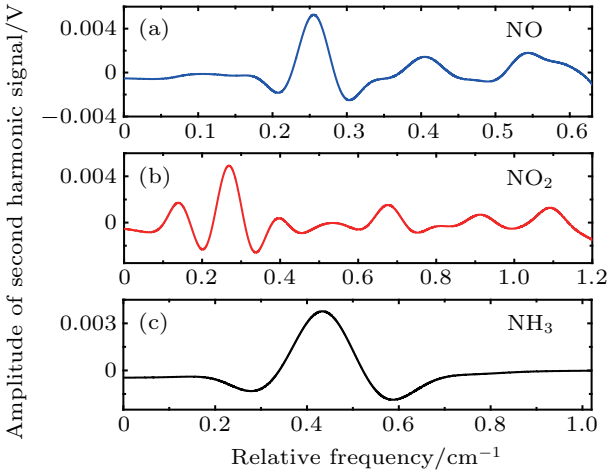



**Fig. 7.** (color online) Measurement examples of $1f$-normalized $2f$ signals of (a) NO, (b) $NO_2$, and (c) $NH_3$ in ambient air.

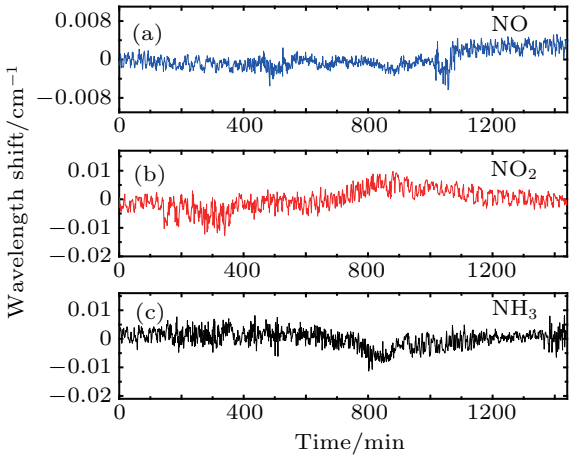



**Fig. 8.** (color online) Wavelength drifts of three QCLs for (a) NO, (b) $NO_2$, and (c) $NH_3$ over 24 hours.

### 4.4. Ambient air monitoring

The long period monitoring of NO, $NO_2$, and $NH_3$ is performed at the urban site of the Jiangsu environmental monitoring center to examine the reliability and accuracy of the prototype. Restricted by the available laboratory space at the experimental site, our prototype is installed in a laboratory on the third floor of the building in a good ventilation condition, whereas a commercial instrument (Teledyne, model T201) is used for comparison and is placed on the sixth floor, which is about 15 meters above the ground. The observation site is beside a street with relatively heavy traffic. To account for the influence of temperature and pressure variations during a long measurement period, the real-time temperature and pressure are measured and used for correcting the absorption line strengths and $2f$ amplitudes of the three target gases. The model T201 used for making comparative measurements is based on chemiluminescence (CL) technology[24] with an external thermal converter to give stable and repeatable NO, $NO_2$, and $NH_3$ measurements. The instrument uses an innovative sample path with specially conditioned materials, to preserve gas samples and minimize the interference. A gas mixing system, together with pure $N_2$ and standard gas samples of NO (10 ppm), $NO_2$ (5 ppm), and $NH_3$ (10 ppm) is used to make daily calibration of the instrument at a sub-ppm level. The detection limit of this instrument is 1 ppb in a 10-min sampling time.

The 24-hour monitoring results of our WMS open-path sensor and the CL reference instrument on November 24, 2016 are shown in Figs. 9–11 for NO, $NO_2$, and $NH_3$ respectively. Data from the reference instrument are averaged hourly by the instrument. The measurement is made by using our WMS instrument every second. The hourly-averaged WMS data are also presented in these figures to illustrate the comparison results. As shown in these figures, the measured NO, $NO_2$, and $NH_3$ concentrations by both instruments reveal that they have the same features and are in good agreement with each other. Compared with the CL instrument, our open-path sensor is able to capture subtle fluctuations of gas concentration with a fast response time of 1 s. Since the location of the open-path sensor is closer to the ground, the rapid fluctuations of gas concentration due to human activities on the street are observed and lead to their rapid changes. The NO concentration shows two high concentration peaks during a day starting at 9 o'clock in the morning and ending at 10 o'clock at night. The $NO_2$ concentration presents an upward trend during the test. Because the $NO_x$ is mainly generated by automobile exhaust and the measuring site is beside the street, a high concentration level in the daytime as well as large concentration changes of NO and $NO_2$ is reasonable. Agricultural activities are the major source of $NH_3$ discharges. The measured $NH_3$ concentration increases from a low value of 4 ppb in the early morning to a value of about 9 ppb in the evening, which decreases back to a low value in the morning.

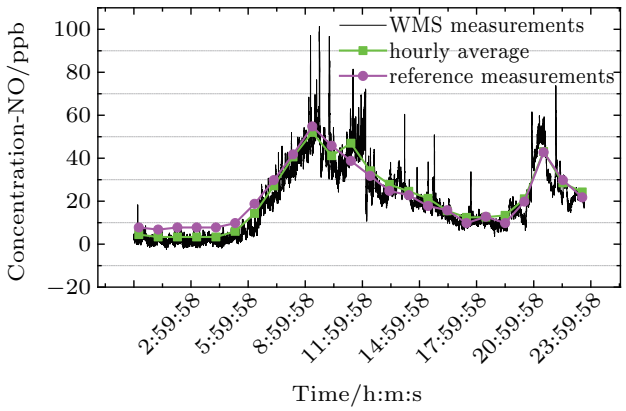



**Fig. 9.** (color online) NO diurnal profiles measured with WMS and CL technologies.

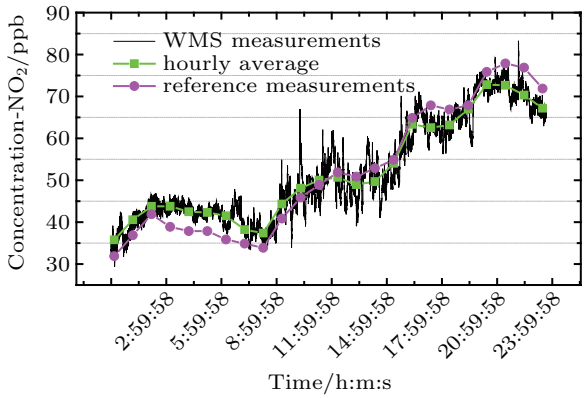



**Fig. 10.** (color online) $NO_2$ diurnal profiles measured with WMS and CL technologies.

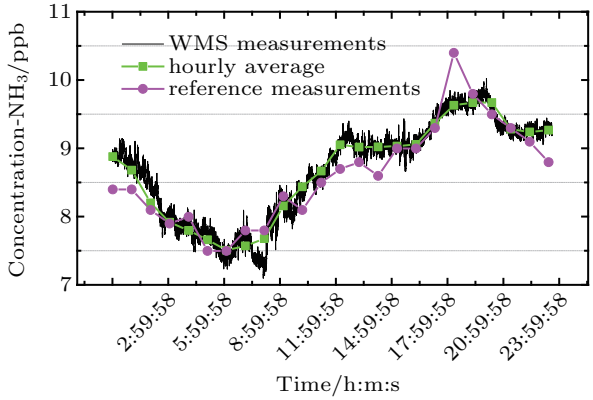



**Fig. 11.** (color online) $NH_3$ diurnal profiles measured with WMS and CL technologies.

For the regression analysis, data from the WMS instrument are block-averaged hourly values in order to match the time resolution of the CL instrument. Figures 12–14 show that the NO, $NO_2$, and $NH_3$ concentrations from the WMS instrument are compared with those from the CL instrument, together with the results of linear regression analysis. Overall, similar trends of concentration changes for target gases between two instruments are observed, where the correlation factor ($R^2$) is larger than 0.85. However, the ratios between the concentrations measured by the two instruments deviate from the ideal ratio of 1:1. The regression line of NO has a slope slightly greater than 1, but has a negative intercept of −1.33 ppb. Relatively high intercept and small slope are found for $NO_2$ as shown in Fig. 13. The $NH_3$ measurements have the lowest correlation factor in the measurements of the three gases. There are several possible reasons for the discrepancies between WMS sensor and CL instrument for three target gases. Firstly, the two instruments sample the ambient air from two nearby but different locations. Secondly, standard gas cylinders of NO, $NO_2$, and $NH_3$ used for calibrating both the instruments are different. Thirdly, measurement error is introduced by the instrument itself. For example, the ambient reactive nitrogen species and the conversion efficiency can lead to the discrepancy between the $NO_x$ concentrations measured by standard CL monitors.[25] Furthermore, due to the strong absorption characteristics of $NH_3$ and the local contamination source on sampling tubing and inlet filters, errors are inevitable for CL ambient data,[26] whereas our open-path WMS instrument is able to directly measure the samples without treating any of them.

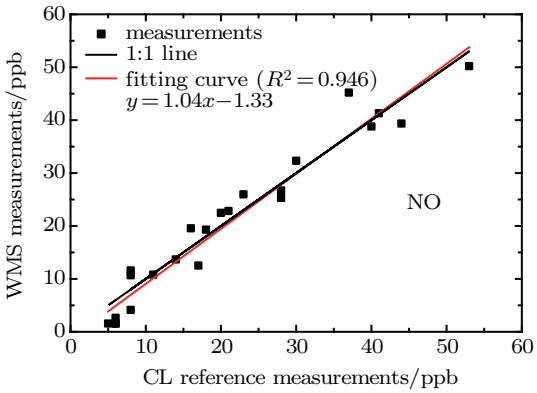



**Fig. 12.** (color online) Scatter NO concentration plots of WMS against CL at 1-hour time resolution, including regression line (red) and 1:1 reference line (black).

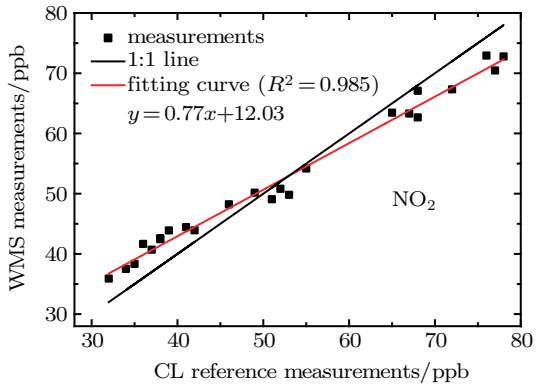



**Fig. 13.** (color online) Scatter $NO_2$ concentration plots of WMS against CL at 1-hour time resolution, including regression line (red) and 1:1 reference line (black).

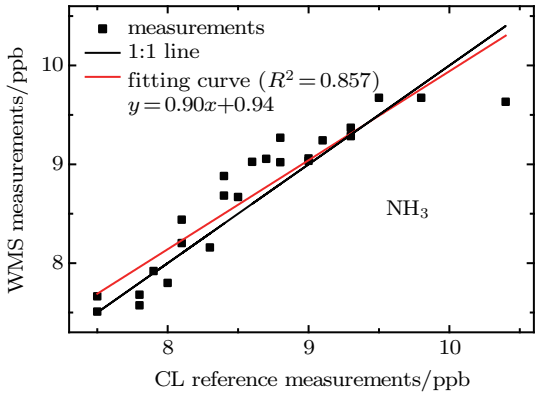



**Fig. 14.** (color online) Scatter $NH_3$ concentration plots of WMS against CL at 1-hour time resolution, including regression line (red) and 1:1 reference line (black).

## 5. Conclusions

By applying the time division multiplexing technique to the WMS, an optical instrument for simultaneously monitor-

ing NO, $NO_2$, and $NH_3$ in the air is developed and demonstrated. To realize the gas detection at a sub-ppb level, the QCLs operating in the mid-infrared wavelength region are used, where the target gases have their stronger absorption lines. The time division multiplexing technology reduces the average light-emitting time of QCLs and the produced heat and improves the thermal stability in continuous operation. The instrument shows an excellent linear response to gas sample concentration over a large range. With an optimum integration time of about 100 s, the detection limit for each of all three gases is less than 0.2 ppb. The measurements are well consistent with the measurements by a commercial CL instrument. It should also be noted that our nondestructive open-path design minimizes the challenges of gas sampling artifacts in contrast to extractive sensors. The stability and reliability of the instrument are tested by field measurements and demonstrate that this detecting system is suitable for real-time monitoring NO, $NO_2$, and $NH_3$ in the air with the advantages of quick response, excellent stability and low minimal detection limit. Our future work will focus on continuous monitoring applications in several cities with different meteorological and geographic conditions for several months. Investigations on the reaction and relation among NO, $NO_2$, and $NH_3$ will also be performed to study their influence on the atmosphere.

## References


[1] Cabot A, Marsal A, Arbiol J and Morante J R 2004 *Sensors and Actuators B* **99** 74

[2] Yang X T, Xie W Q and Yuan Z G 2016 *Optik* **127** 3788

[3] Dong L, Spagnolo V, Lewicki R and Tittel F K 2011 *Opt. Express* **19** 24037

[4] Peng W Y, Sur R, Strand C L, Spearrin R M, Jeffries J B and Hanson R K 2016 *Appl. Phys. B* **122** 188

[5] He Y, Jin C J, Kan R F, Liu J G, Liu W Q, Hill J, Jamie I M and Orr B J 2014 *Opt. Express* **22** 13170

[6] Shadman S, Rose C and Yalin A P 2016 *Appl. Phys. B* **122** 194

[7] Xia H, Dong F Z, Wu B, Zhang Z R, Pang T, Sun P S, Cui X J, Han L and Wang Y 2015 *Chin. Phys. B* **24** 034204

[8] Andersson M, Persson L, Svensson T and Svanberg S 2007 *Rev. Sci. Instrum.* **78** 113107

[9] Mei L and Svanberg S 2015 *Appl. Opt.* **54** 2234

[10] Qu D S, Hong Y J, Wang G Yand Pan H 2017 *Chin. Phys. B* **26** 064204

[11] Liu C W, Zhang J C, Yan F L, Jia Z W, Zhao Z B, Zhuo N, Liu F Q and Wang Z G 2017 *Chin. Phys. Lett.* **34** 034209

[12] Zhao Y, Zhang J C, Jia Z W, Liu Y H, Zhuo N, Zhai S Q, Liu F Q and Wang Z G 2016 *Chin. Phys. Lett.* **33** 124201

[13] Tuzson B, Zeyer K, Steinbacher M, McManus J B, Nelson D D, Zahniser M S and Emmenegger L 2013 *Atmos. Meas. Tech.* **6** 927

[14] Wang Y, Nikodem M, Zhang E, Zhang E, Cikach F, Bames J, Comhair S, Kao G and Wysocki G 2015 *Sci. Rep.* **5** 9096

[15] Jágerská J, Jouy P, Tuzson B, Looser H, Mangold M, Soltic P, Hugi A, Brönnimann R, Faist J and Emmenegger L 2015 *Opt. Express* **23** 1512

[16] Panella B, Maas D, Brändle H and Galletti B 2013 *Optical Instrumentation for Energy and Environmental Applications*, (November 3–7, 2013, Tucson, USA), in *Renewable Energy and the Environment*, OSA Technical Digest (OSA, 2013), paper EW1A.3

[17] Owen K and Farooq A 2014 *Appl. Phys. B* **116** 371

[18] Miller D J, Sun K, Tao L, Khan M A and Zondlo M A 2014 *Atmos. Meas. Tech.* **7** 81

[19] Wei M, Ye Q H, Kan R F Chen B, Yang C G, Xu Z Y, Chen X, Ruan J, Fan X L, Wang W, Hu M and Liu J G 2016 *Chin. Phys. B* **25** 094210

[20] Chinese Ministry of Environmental Protection 2013 National Environmental Standard HJ654-2013

[21] Werle P O, Mücke R and Slemr F 1993 *Appl. Phys. B* **57** 131

[22] Sanchez N P, Yu Y, Dong L, Griffin R and Tittel F K 2016 *Proc. SPIE* **9755** 975508

[23] Pakmanesh N, Cristescu S M and Ghorbanzadeh A, Harren F J M and Mandon J 2016 *Appl. Phys. B* **122** 10

[24] Villena G, Bejan I, Kurtenbach R, Wiesen P and Kleffmann J 2012 *Atmos. Meas. Tech.* **5** 149

[25] Dunlea E J, Herndon S C, Nelson D D, Volkamer R M, San Martini F, Sheehy P M and Allwine E J 2007 *Atmos. Chem. Phys.* **7** 2691

[26] Williams E J, Sandholm S T, Bradshaw J D, Schendel J S, Langford A O, Quinn P K, LeBel P J, Vay S A, Roberts P D, Norton R B, Watkins B A, Buhr M P, Parrish D D, Calvert J G and Fehsenfeld F C 1992 *J. Geophys. Res.* **97** 11591